Characterization of the Tryptophan Tryptophyl-Semiquinone Catalytic Intermediate of Methylamine Dehydrogenase by Electron Spin−Echo Envelope Modulation Spectroscopy

Vinita Singh, Zhenyu Zhu,† Victor L. Davidson,† and John McCracken*

Contribution from the Department of Chemistry, Michigan State University, East Lansing, Michigan 48824, and Department of Biochemistry, University of Mississippi Medical Center, Jackson, Mississippi 39216

Received September 20, 1999. Revised Manuscript Received December 2, 1999

Abstract: The electronic structure of the tryptophan tryptophyl-semiquinone (TTQ•) cofactor generated by addition of the substrate, methylamine, to methylamine dehydrogenase (MADH) from *Paracoccus denitrificans* has been studied by continuous-wave electron paramagnetic resonance (cw-EPR) and electron spin−echo envelope modulation (ESEEM) spectroscopy. The cw-EPR spectrum of TTQ semiquinone prepared by substrate addition (N-form) was found to differ substantially from that observed when the semiquinone was generated by dithionite reduction of the enzyme (O-form). These differences prompted a detailed study of hyperfine and nuclear quadrupole interactions of the three ^{14}N atoms of the semiquinone species using ESEEM. Two of these heteroatoms are derived from the indole and indole−quinone side chains that comprise TTQ, while the third ^{14}N originates from substrate methylamine. Three-pulse ESEEM spectra of the $CH_3{}^{14}NH_2$-reduced sample showed three isolated features at 1.0, 1.5, and 4.3 MHz, which were absent in the MADH sample reduced with $CH_3{}^{15}NH_2$. Analysis of the spectral data for substrate-derived ^{14}N revealed an isotropic hyperfine coupling of 2.4 MHz and nuclear quadrupole couplings characterized by $e^2qQ = 1.7$ MHz and $\eta = 0.5$. The hyperfine and the nuclear quadrupole couplings found for the two ^{14}N nuclei indigenous to TTQ were: A_{iso}, 2.8 and 1.9 MHz; e^2qQ, 3.0 and 2.1 MHz and η, 0.3 and 0.7, respectively. Taken together, these couplings provide definitive evidence that substrate ^{14}N is covalently bound to TTQ when the cofactor is in its one-electron reduced form and that it has an imine-like structure. The intensities of the modulations indicate that the semiquinone generated by the method recently reported by Zhu and Davidson (*Biochim. Biophys. Acta* **1998**, *1364*, 297−300) results in a homogeneous preparation of the radical. A comparison of the ^{14}N hyperfine and nuclear quadrupole couplings measured for the N-form semiquinone with those measured previously for O-form (Warncke, K.; Brooks, H. B.; Lee H.-I.; McCracken, J.; Davidson, V. L.; Babcock, G. T. *J. Am. Chem. Soc*. **1995**, *117*, 10063−10075) shows that a significant change occurs in the highest occupied molecular orbital when substrate nitrogen is bound, and may be related to the different redox and electron-transfer properties of these two semiquinone forms.

Introduction

Methylamine dehydrogenase (MADH) catalyzes the oxidative deamination of methylamine to yield formaldehyde and ammonia as written below:

$$CH_3NH_2 + 2\,H_2O + 2\,\mathrm{Ami}(Cu^{2+}) \rightarrow HCHO + NH_4{}^+ + H_3O^+ + 2\,\mathrm{Ami}(Cu^+)$$

This is the first step in the assimilation of methylamine, which serves as a carbon source for methylotrophic bacteria. During this reaction, two electrons are transferred from substrate methylamine to amicyanin (Ami in the above equation), a type I blue copper protein of molecular weight 11.5 kDa, which mediates electron transfer from MADH to *c*-type cytochromes.[1−4] The native enzyme is void of metal ion cofactors and has an overall $\alpha_2\beta_2$ subunit structure[5,6] with subunit molecular masses of 43 and 14 kDa, respectively. The smaller subunits each contain a covalently bound quinone cofactor. The cofactor structure common to MADH from different species was identified by chemical and spectroscopic methods,[7] and confirmed by X-ray crystallographic analyses[8] to be 2′,4-bitryptophan-6,7-dione, or tryptophan tryptophylquinone (TTQ, Figure 1). TTQ is derived from posttranslational modification of the side-chains of two tryptophan residues, Trp108 and Trp57, which are linked by a covalent bond between C2 of Trp108 and C4 of Trp57. In addition, the indole of Trp57 is oxidized to an ortho-quinone at the C6 and C7 positions. The indole and

* To whom correspondence should be addressed. Telephone: 517-355-9715, ext. 269. Fax: 517-353-1793. E-mail: mccracke@msu.edu.
† University of Mississippi Medical Center.

(1) Tobari, J.; Harada, Y. *Biochim. Biophys. Res. Commun.* **1981**, *101*, 502.
(2) van Houwelingen, T.; Canters, G. W.; Stobbelaar, G.; Duine, J. A.; Frank, J. J.; Tsugita, A. *Eur. J. Biochem.* **1985**, *153*, 75.
(3) Husain, M.; Davidson, V. L. *J. Biol. Chem.* **1985**, *260*, 14626.
(4) Lawson, S. A.; Anthony, C. *Biochem. J.* **1985**, *228*, 719.
(5) Chen, L.; M., D.; Durley, R. C.; Y., C. A.; E., L. M.; Davidson, V. L.; Mathews, F. S. *J. Mol. Biol.* **1998**, *276(1)*, 131−49.
(6) Chen, L.; Durley, R. C.; Davidson, V. L.; Mathews, F. S. *Science* **1994**, *264*, 86−89.
(7) McIntire, W. S.; Christoserdov, A. Y.; Wemmer, D. E.; Lidstrom, M. E. *Science* **1991**, *252*, 817−824.
(8) Chen, L.; Mathews, F. S.; Davidson, V. L.; Huizenga, E. G.; Vellieux, F. M. D.; Duine, J. A.; Hol, W. G. J. *FEBS Lett.* **1991**, *287*, 163−166.

10.1021/ja9934246 CCC: $19.00
Published on Web 01/21/2000

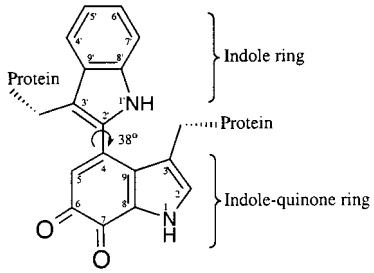

Figure 1. Structure of the oxidized TTQ cofactor of MADH.

indole−quinone rings of oxidized TTQ are not coplanar, but are at a dihedral angle of 38°.[5] Crystal structures have been determined for isolated *Paracoccus denitrificans* MADH and for the MADH−amicyanin complex which shows a composition of $\alpha_2\beta_2$Amicyanin$_2$.[6] The modified tryptophylquinone side chain of Trp57 is located in a hydrophobic channel between α and β subunits with the C6 carbonyl group accessible to solvent and the C7 carbonyl hydrogen-bonded to an amide hydrogen on the peptide backbone.[5] The phenyl portion of the indole side chain of Trp108 breeches the surface of the β-subunit and is only 9.3 Å from the Cu site of amicyanin when the MADH−amicyanin complex is formed. Thus, TTQ is able to serve as a bridge between the chemical reactions, which occur in the enzyme active site, and the electron-transfer reactions that occur from the enzyme surface. Furthermore, since TTQ catalyzes a two-electron oxidation of substrate and then donates electrons to a one-electron carrier, the semiquinone form of TTQ is a critical reaction intermediate.

The catalytic mechanism of MADH can be divided into discrete reductive and oxidative half reactions. In the reductive half (Figure 2a), methylamine reacts with TTQ at the C6 carbonyl carbon to form an aminoquinol (N-quinol) species.[9] In the subsequent oxidative half reaction (Figure 2b), two electrons are transferred sequentially from the substrate-reduced MADH to amicyanin.[5] Studies on the pH dependence of the redox potentials of MADH[10] have shown that the quinol is singly protonated and that the semiquinone is anionic and unprotonated. Thus, the two-electron oxidation of fully reduced MADH is linked to transfer of a single proton, which occurs in the conversion of the fully reduced quinol to the semiquinone form (Figure 2b). It was shown using rapid scanning stopped-flow spectroscopy[11] that the oxidation of the N-semiquinone by amicyanin occurs by a sequential mechanism in which oxidation to an iminoquinone precedes hydrolysis and release of ammonia. However, in the presence of excess of substrate (i.e., the steady state), methylamine rather than water initiates a nucleophilic attack at the C6 position to release ammonia and form the next TTQ−substrate imine adduct. Given the critical physiologic role of the N-semiquinone in the catalytic cycle of MADH, it is important to understand its electronic properties.

Observation of a metastable semiquinone intermediate during controlled in vitro oxidation of substrate-reduced MADH was reported by Davidson et al. (1990)[12] and supported by previous pulsed EPR studies.[13] For these studies, TTQ semiquinone was formed by comproportionation of a 1:1 molar mixture of oxidized and substrate-reduced TTQ cofactors that resulted from addition of a 0.5 molar equivalent of substrate to the resting enzyme.[12] As a result, enzyme samples contained a mixture of N- and O-form semiquinones. The resulting ESEEM spectra clearly showed ^{14}N modulations from methylamine-derived nitrogen. Because the intensities of these ^{14}N modulations were similar to those found for the heteroatoms of TTQ$^{\bullet}$, the authors concluded that methylamine derived ^{14}N was covalently bound to TTQ$^{\bullet}$ and that NH_3 release must take place after or in concert with oxidation of the TTQ semiquinone.[13] These results generated considerable controversy.

The presence of a substrate-derived nitrogen atom covalently bound to TTQ was questioned by Gorren et al.[14,15] and Kuusk and McIntire[16] on the basis of their studies of the effects of alkali metal cations and ammonium and alkylammonium cations on the absorption, resonance Raman, and EPR spectra of the oxidized and semiquinone forms of MADH. Resonance Raman spectra of oxidized MADH showed that the changes induced by the addition of a 10^4-10^6 molar excess of these cations resulted from noncovalent interactions with the carbonyl oxygens of TTQ. These results led Gorren and co-workers[15] to point out that MADH may function via an imine elimination mechanism without covalent binding between methylamine and TTQ. These authors also suggested that the ^{14}N-ESEEM detected by Warncke et al.[13] could have originated from a through-space magnetic coupling with noncovalently bound ammonia in the active site, casting doubt on the mechanistic conclusions of the earlier work. Subsequent ^{15}N NMR studies by Bishop et al.[17] substantiated that the substrate-reduced MADH does possess a substrate-derived nitrogen that is covalently bound to TTQ. Kinetic studies of the oxidation of this substrate-reduced MADH by amicyanin[18] demonstrated that the N-form semiquinone is a true physiological reaction intermediate which accumulates during two sequential one-electron oxidations of reduced MADH by amicyanin.

The pulsed EPR method of electron spin−echo envelope modulation (ESEEM) is well suited for the measurement of the weak hyperfine couplings which characterize the interaction of substrate-derived nitrogen with TTQ. Unfortunately, the comproportionation procedure employed for the preparation of N-form semiquinone in the earlier study by Warncke et al.[13] yielded a mixture of N- and O-form TTQ radicals. As a result, although the ESEEM spectra clearly showed differences due to isotopic substitution of the methylamine nitrogen, differences in the electronic structures of these two radicals gave rise to a spectral complexity that prevented analysis of the early ESEEM data by numerical simulation. In this paper, the ^{14}N-ESEEM for substrate-reduced MADH is reexamined, using samples poised in the semiquinone state by a new photooxidation procedure that involves stoichiometric addition of substrate and illumination at 320−380 nm. These new data allowed a detailed analysis of substrate-derived and indole-based ^{14}N-hyperfine couplings. The results support and extend the original conclusion of Warncke et al.[13] regarding substrate binding to TTQ. They also verify that this new poising procedure yields a pure N-form semiquinone, and they provide additional new evidence for the formation of an imino-semiquinone intermediate before the release of ammonia.[11] The new ESEEM data also provide information on the chemical structure of the substrate-derived

(9) Huizinga, E. G.; Zanteen, B. A. M.; Duine, J. A.; Jongejan, J. A.; Hullema, F.; Wilson, K. S.; Hol, W. G. J. *Biochemistry* **1992**, *31*, 9789.
(10) Zhu, Z.; Davidson, V. L. *J. Biol. Chem.* **1998**, *273*, 14254−14260.
(11) Zhu, Z.; Davidson, V. L. *Biochemistry* **1999**, *38*, 4862−4867.
(12) Davidson, V. L.; Jones, L. H.; Kumar, M. A. *Biochemistry* **1990**, *29*, 10786−10791.
(13) Warncke, K.; McCracken, J.; Brooks, H. B.; Babcock, G. T.; Davidson, V. L. *J. Am. Chem. Soc.* **1993**, *115*, 63−64.
(14) Gorren, C. F. A.; Duine, J. A. *Biochemistry* **1994**, *33*, 12202−12209.
(15) Gorren, C. F. A.; Moenne-Loccoz, P.; Backes, G.; Vries, S.; Loehr, J. S.; Duine, J. A. *Biochemistry* **1995**, *34*, 12926−12931.
(16) Kuusk, V.; McIntire, W. S. *J. Biol. Chem.* **1994**, *269*, 26136−26143.
(17) Bishop, G. R.; Valente, E. J.; Whitehead, T. L.; Brown, K. L.; Hicks, R. P.; Davidson, V. L. *J. Am. Chem. Soc.* **1996**, *118*, 12868−12869.
(18) Bishop, G. R.; Brooks, H. B.; Davidson, V. L. *Biochemistry* **1996**, *35*, 8948−8954.

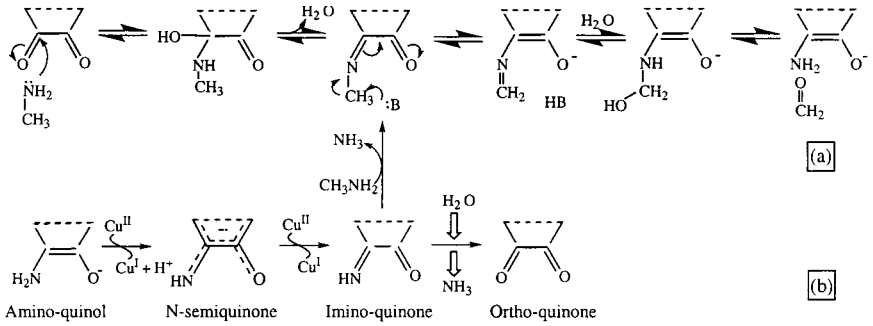

Figure 2. Proposed reaction pathway for MADH divided into reductive (a) and oxidative (b) steps.

nitrogen bound to the TTQ semiquinone, and its protonation state and extent of hydrogen bonding in the enzyme active site. These data are correlated with results of kinetic and structural studies of MADH. The ESEEM results also show a striking difference between the electronic structures of N-form semiquinone and the nonphysiologic O-form semiquinone that is generated by chemical reduction with dithionite.[19] This is discussed in relation to the observation that the N- and O-forms of MADH behave very differently with respect to their electron-transfer reactions with amicyanin.[10]

Materials and Methods

Protein Purification and Preparation. The MADH under study was obtained from *P. denitrificans* and was purified as described previously.[3] The concentration of MADH was calculated from known extinction coefficients[3,20] in 10 mM phosphate buffer, pH 7.5. The extinction coefficients of the different redox forms of MADH vary with pH and ionic composition of the buffer.[15] MADH was fully reduced with substrate methylamine (1 MADH:2 methylamine). Then the fully reduced MADH, which exhibits an absorption maximum at 330 nm, was photooxidized by exposing it to a source of long-range UV light until the absorption at 420 nm (due to the semiquinone form) reached a maximum.[21] This typically occurred in 5−10 min. The source for long-range UV light was a Rad-Free RF UV-365 long-wave UV lamp (Schleicher & Schleicher) using an 8 W bulb that emitted light-spanning wavelengths from 320 to 380 nm with a peak value at 365 nm. The UV light source was placed approximately 3 in. away from the sample contained in a quartz cuvette. The effects of light are completely reversible.[21]

Continuous-Wave EPR Spectroscopy. CW-EPR spectra were obtained at X-band on a Bruker ESP300E EPR spectrometer, using a TE_{102} EPR cavity, an Oxford ESR-900 continuous flow cryostat and an ITC 502 temperature controller. The microwave frequency was monitored by an EIP Microwave model 25B frequency counter, and the static magnetic field strength was measured using a Bruker ER 035M NMR gaussmeter.

ESEEM Spectroscopy. The ESEEM spectra were recorded at X-band with a home-built spectrometer[22] using a sample probe that employed a folded strip-line resonator[23] and the Gordon coupling scheme described by Britt and Klein.[24] Our spectrometer was modified from its original design in that signal averaging and subsequent integration of the electron spin−echo signals was accomplished by a Tektronix 620 B digital oscilloscope fed directly by the double-balanced mixer and mixer preamplifier of the microwave bridge. The pulse sequence for the three-pulse ESEEM experiment, $\pi/2-\tau-\pi/2-T-\pi/2-\tau$-echo, used a two-step (0, 0, 0), (π, π, 0) microwave pulse phase cycling to eliminate two-pulse echo interference. The modulation was observed by recording integrated spin−echo intensities as a function of T. ESEEM spectra were recorded at τ values that ranged from 150 to 600 ns. Typical conditions for data collection were: microwave frequency, 8.815 GHz; pulse power, 43 W; pulse width, 20ns (fwhm); sequence repetition rate, 6 Hz; total number of experimental points, 512; time increment, 20 ns; number of events averaged/point, 10; sample temperature, 4.2 K; each data set represented an average of 9 scans.

ESEEM spectra were obtained by a Fourier analysis procedure that included dead time reconstruction.[25] Numerical simulations of the experimental data were performed on Sun SparcII work station. Simulation programs were written in FORTRAN and were based on the density matrix formalism developed by Mims.[26] Software for the frequency analysis of the experimental and simulated data was written in Matlab (Mathworks, Nantick, MA). The data collection programs for our pulsed EPR spectrometer were written in LabVIEW 5.0.1 (National Instruments) running on a Power Computing model 200 Power PC.

Results

CW-EPR Spectroscopy. Figure 3 shows continuous wave EPR spectra of TTQ semiquinone prepared by reduction of MADH with dithionite (3a), $CH_3{}^{14}NH_2$ (3b), and $CH_3{}^{15}NH_2$ (3c) in frozen buffer. All three spectra consist of simple derivative line shapes that have no observable hyperfine structure. The dithionite-reduced (O-form) and the substrate-reduced (N-form) semiquinone spectra are centered at $g = 2.0043$ and $g = 2.0039$, respectively. The peak-to-peak line widths of the O-form, ^{14}N-, and ^{15}N-substrate generated semiquinones were observed to be 6.81G, 11.09, and 11.55G, respectively. The line shapes for all three of these TTQ semiquinones are more symmetrical than those found for samples poised by comproportionation.[13] Apparently, the asymmetry observed previously for the comproportionation products arose from the mixture of O- and N-form spectra present.[19]

ESEEM Spectroscopy. To understand the differences in electronic structure of substrate- and dithionite-poised semiquinone, ESEEM spectroscopy was used to probe the hyperfine couplings of ^{14}N nuclei derived from substrate and from those native to the cofactor. Typically, three-pulse ESEEM data were characterized by deep low-frequency modulations that damped over a 10 μs range of T (Figure 4a, inset). A cosine Fourier transformation of the time domain ESEEM data collected at $\tau = 219$ ns, for N-form semiquinone poised with ^{14}N-methylamine yielded the spectrum of Figure 4a. This spectrum shows sharp features in the low-frequency region, at 0.5, 1.0, 1.5, 2.0, and 2.5 MHz and a broad feature with a complex line shape from 4.6 to 5.8 MHz. To distinguish peaks that arise from substrate ^{14}N-coupling, data were collected under identical spectrometer

(19) Warncke, K.; Brooks, H. B.; Lee, H.-I.; McCracken, J.; Davidson, V. L.; Babcock, G. T. *J. Am. Chem. Soc.* **1995**, *117*, 10063−10075.
(20) Husain, M.; Davidson, V. L.; Gray, K. A.; Knaff, D. B. *Biochemistry* **1987**, *26*, 4139−4143.
(21) Zhu, Z.; Davidson, V. L. *Biochim. Biophys. Acta* **1998**, *1364*, 297−300.
(22) McCracken, J.; Shin, D.-H.; Dye, J. L. *Appl. Magn. Reson.* **1992**, *3*, 305−316.
(23) Lin, C. P.; Bowman, M. K.; Norris, J. R. *J. Magn. Reson.* **1985**, *65*, 369−374.
(24) Britt, R. D.; Klein, M. P. *J. Magn. Reson.* **1987**, *74*, 535−540.
(25) Mims, W. B. *J. Magn. Reson.* **1984**, *59*, 291−306.
(26) Mims, W. B. *Phys. Rev. B: Solid State* **1972**, *5*, 2409−2419.

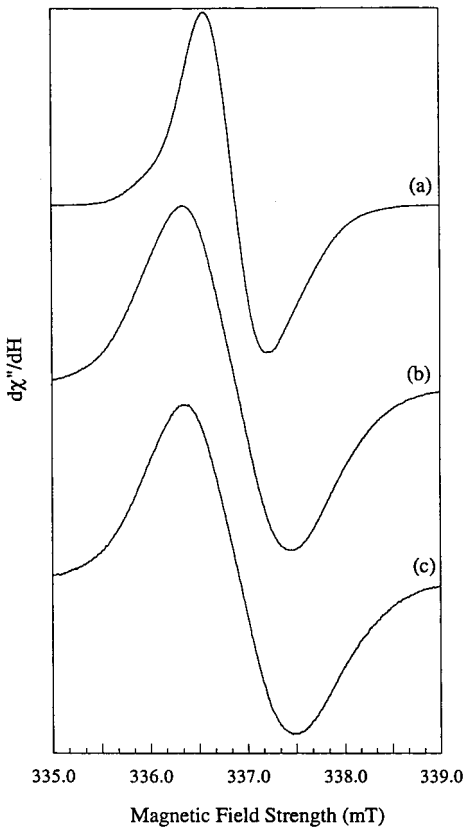

Figure 3. Continuous-wave EPR spectra of the semiquinone forms of methylamine dehydrogenase from *P. denitrificans* generated by dithionite addition (O-form) (a), ^{14}N-methylamine addition followed by illumination (b), and ^{15}N-methylamine addition followed by illumination. Spectra were collected under the following conditions: microwave power, 0.63 mW; microwave frequency, 9.473 GHz; modulation frequency, 100 kHz; modulation amplitude, 0.1 mT; sample temperature, 103 K; and number of scans averaged, 10.

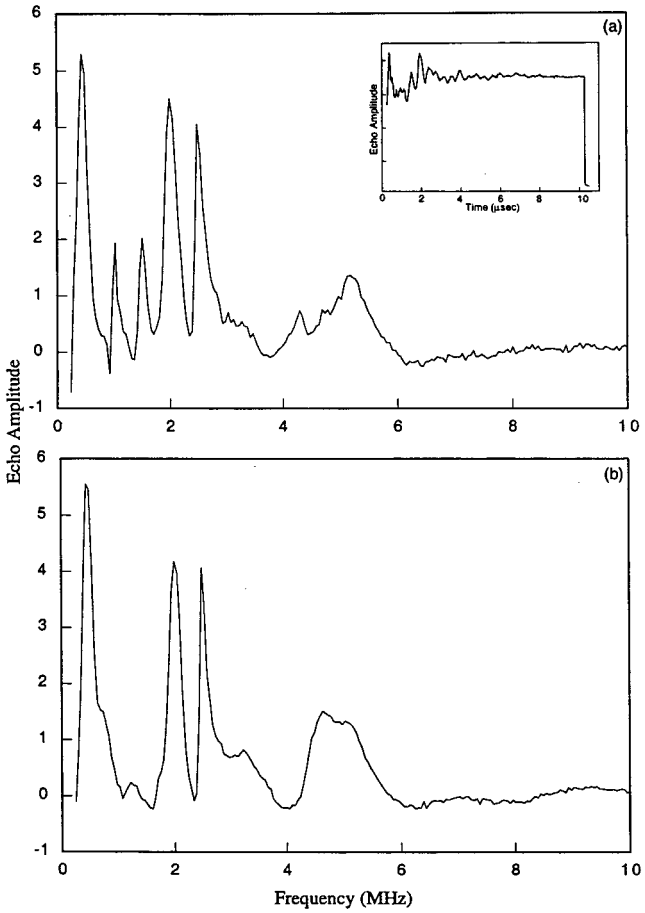

Figure 4. Frequency-domain three-pulse ESEEM spectra of randomly oriented (a) ^{14}N-methylamine-reduced semiquinone; inset, corresponding time-domain data; (b) ^{15}N-methylamine-reduced semiquinone. Conditions: τ, 219 ns; microwave frequency, 8.815 GHz; magnetic field, 315.5 mT; microwave pulse power, 43 W; pulse sequence repetition rate, 4 Hz; events averaged per time point, 10; sample temperature, 4.2 K; number of scans averaged, 9.

conditions for ^{15}N-methylamine poised semiquinone and are shown in Figure 4b. This spectrum also features deep modulations with peaks at 0.5, 2.0, and 2.5 MHz characterized by narrow line shapes, along with a broad feature at 4.5−5.8 MHz. The spectra in Figure 4 are indicative of nitrogen nuclei coupled to a paramagnetic center near the "exact cancellation condition"[27,28] that arises when the isotropic hyperfine interaction is equal to twice the nuclear Zeeman frequency, $|A_{iso}| = 2\nu_n$. Under these conditions, the hyperfine and nuclear Zeeman interactions "cancel" one another in one of the electron spin manifolds, so that the modulation frequencies are dominated by the ^{14}N-nuclear quadrupole interaction. This manifold yields three narrow, low-frequency peaks in the ESEEM spectra where the two lower frequencies combine to give the third. The other electron spin manifold gives rise to broad, or rapidly damped ESEEM features with the most prominent spectral component being that between the highest and lowest energy levels of the manifold. Because the two energy levels involved in this modulation component have mostly $m_I = 1$ or $m_I = -1$ character, this peak is referred to as a "double quantum" feature. The frequency of this broad component at exact cancellation is roughly four times the nuclear Larmor frequency, or 4 MHz in the case of ^{14}N at X-band. Because ^{15}N is a spin $I = {}^1/_2$ nucleus, it does not have a quadrupole moment, and its ESEEM is determined by hyperfine and nuclear Zeeman interactions only.

A comparison of the two data sets shown in Figure 4 identifies the narrow peaks at 1.0 and 1.5 MHz as arising from hyperfine coupling to the $CH_3{}^{14}NH_2$-derived nitrogen.

Figure 5 shows three-pulse ESEEM data collected for $CH_3{}^{14}NH_2$- and $CH_3{}^{15}NH_2$-treated MADH at two other τ-values, 365 ns (Figure 5a, b) and 450 ns (Figure 5c, d). Because of the τ dependence of three-pulse ESEEM amplitudes, different frequencies are accentuated in these two data sets. For the $\tau =$ 365 ns data (Figure 5a, b), there is a significant difference in the amplitude of the 0.5 MHz component, with it being twice as intense with respect to the 2.0 and 2.5 MHz peaks (assigned to TTQ) for the $CH_3{}^{14}NH_2$ sample as for the $CH_3{}^{15}NH_2$ counterpart. This observation allows us to assign part of the intensity at 0.5 MHz to substrate-derived ^{14}N. Similarly, peaks at 0.8 and 1.2 MHz are observed for both ^{14}N- and ^{15}N-methylamine-treated samples at $\tau = 450$ ns (Figure 5a, b) and are assigned to the second ^{14}N of the TTQ cofactor (N(2)). ESEEM data collected at $\tau = 365$ and 450 ns show a strong peak at 4.3 MHz due to substrate-derived ^{14}N. The narrow line width of this modulation component relative to the broad 4.6−5.8 MHz feature observed for N(1) of the TTQ$^{\bullet}$ (Figure 4a, b) indicates that the anisotropy in the hyperfine interaction for substrate-derived ^{14}N might be comparatively small. Assignments based on these observations and the assumption that both

(27) Mims, W. B.; Peisach, J. *J. Chem. Phys.* **1978**, *69*, 4921−4930.
(28) Flanagan, H. L.; Singel, D. J. *J. Chem. Phys.* **1987**, *87*, 5606−5616.

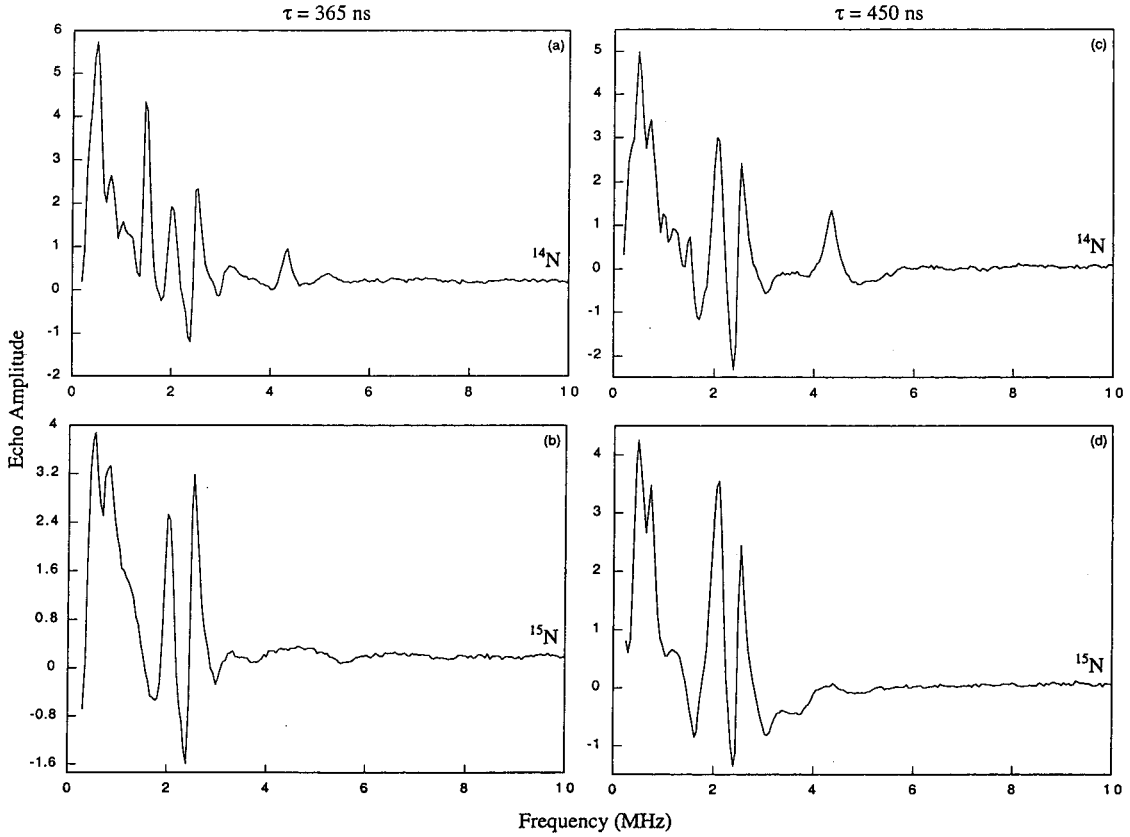

Figure 5. Three-pulse ESEEM spectra of randomly oriented ^{14}N-methylamine-reduced semiquinone (a) and (c); and ^{15}N-methylamine-reduced semiquinone (b) and (d). For traces (a) and (b), $\tau = 365$ ns; and for (c) and (d), $\tau = 450$ ns. Other conditions were identical to those given in Figure 4.

Table 1: ^{14}N ESEEM Frequencies and Simulation Results[a]

^{14}N nucleus	ESEEM freq. (MHz)	$A_\perp$	$A_{\|\|}$	A_{iso}	A_{dip}	e^2qQ/h	η	α (deg)	β (deg)	γ (deg)
substrate	0.5, 1.0, 1.5, 4.3	2.1	3.1	2.4	0.3	1.7	0.5	0	108	60
N(1)−TTQ	0.5, 2.0, 2.5, 4.8−5.1	2.6	3.2	2.8	0.2	3.0	0.3	0	69	0
N(2)−TTQ	0.8, 1.2	1.4	3.0	1.9	0.5	2.1	0.7	0	0	0
N(1) O-form[b]	0.4, 2.1, 2.5, 4.0−6.0	1.9	2.6	2.1	0.3	3.0	0.2	0	60	0
N(2) O-form[b]	0.8, 1.8, 3.1, 5.0−6.0	1.2	2.1	1.5	0.3	3.2	0.6	0	90	0

[a] All hyperfine couplings and e^2qQ values are given in MHz. [b] Data taken from ref 19.

TTQ nitrogens (labeled N-1 and N-2) are near exact cancellation such that their low-frequency lines are additive, are listed in Table 1.

Discussion

The observed increase in peak-to-peak line width of the cw-EPR spectra for substrate-reduced as compared to dithionite-reduced semiquinone is indicative of a different electronic structure for the two forms. To understand these differences in detail, the hyperfine and quadrupole coupling constants for the nitrogens that give rise to the ESEEM of Figures 4 and 5 must be determined. The analysis of ^{14}N ESEEM spectra involves eight adjustable spin Hamiltonian parameters for each nucleus: three principal elements for the hyperfine tensor; the quadrupole coupling constant, e^2qQ/h, and its asymmetry parameter, η; and three Euler angles relating the orientation of the quadrupole tensor's principal axis system to that of the hyperfine tensor. Because the substrate-derived ^{14}N and N(1) of TTQ are likely near exact cancellation, good starting values for e^2qQ, η, and $A_{iso} = {}^1/_3(A_{||} + 2A_\perp)$ can be determined directly. Also, the assumption of an axial ^{14}N-hyperfine tensor reduces the number of parameters for each ^{14}N by one. Our simulations are then mostly aimed at determining the hyperfine anisotropy, $A_{dip} = {}^1/_3(A_{||} - A_\perp)$, and the Euler angles that relate the two tensors. These parameters manifest themselves in the spectra of Figures 4 and 5 in that they control the line shapes of broad peak in the 4−6 MHz region and influence the τ-suppression behavior of the ESEEM spectra. Our numerical simulations focused on accounting for the frequencies, line shapes, and relative amplitudes of the peaks and then on understanding the changes that occurred as τ was varied.

The frequencies of the peaks assigned as "pure" nuclear quadrupole resonances at exact cancellation are given by, $\nu_0 = (e^2qQ)\eta/2$, $\nu_- = e^2qQ(3 - \eta)/4$, and $\nu_+ = e^2qQ(3 + \eta)/4$; hence, $e^2qQ = 2(\nu_+ + \nu_-)/3$; and $\eta = 3(\nu_+ - \nu_-)/(\nu_+ + \nu_-)$. Using these equations, the nqi parameters for the substrate-derived ^{14}N nitrogen are estimated to be: e^2qQ, 1.7 MHz; and η, 0.6. Similarly for the N(1) nitrogen of TTQ, $e^2qQ = 3.0$ MHz and $\eta = 0.3$. When the anisotropic hyperfine interaction is small, A_{iso} can be estimated from the frequency of the double quantum peak, ν_{dq}, that arises from the electron spin manifold where Zeeman and hyperfine fields are additive, using the following equation: $A_{iso}^2/4 \mp \nu_n A_{iso} + (e^2qQ/4)^2\,(3 + \eta^2) + \nu_n^2 - \nu_{dq}^2/4 =$

0.[29] Using the values of e^2qQ and η determined above, A_{iso} values of 2.1 and 6.1 MHz and 2.5 and 6.5 MHz, respectively, were estimated for the substrate-derived ^{14}N and N(1) of TTQ. The higher values of A_{iso} were neglected because they are far from the exact cancellation value of A_{iso}, 1.94 MHz at 3155 G.

Using these initial estimates for nuclear quadrupole and isotropic hyperfine coupling constants along with nonadjustable parameters dictated by our experimental conditions, computer simulations of the data shown in Figures 4 and 5 were undertaken. The ESEEM spectrum of each nitrogen was first simulated separately and then combined using the product rule.[30] The Euler angles were initially set to zero, and the estimated values of e^2qQ and η were varied to account for the positions of the narrow, low-frequency components whose characteristics are primarily determined by the nuclear quadrupole interaction. Then, hf tensor values were varied to obtain the correct position and width of the double quantum line. Finally, the Euler angles were varied to account for the relative intensities of the low-frequency components and shape of the double quantum peak. As the line shape of the double quantum feature depends on the hf tensor principal values as well as on Euler angles, they had to be adjusted simultaneously in order to obtain the best fit to the data.

Only two ^{14}N features at 0.8 and 1.2 MHz from the second indole nitrogen N(2) of TTQ$^{\bullet}$ are resolved (Figure 5c). It is possible that these two frequencies represent ν_0 and ν_- for N(2) and that ν_+ could overlap with ν_- from N(1) at 2.0 MHz. With this assumption, simulations were carried out using the above procedure. Because the "double quantum" peak from this nitrogen was not resolved at any of the τ values studied, we focused on simulations that showed small ν_{dq} amplitudes for this nucleus, presumably because of larger hf anisotropy than that characterizing N(1) or substrate-derived nitrogen. The other possibility, that ν_{dq}'s from both N(1) and N(2) fall in the 4.6−5.8 MHz region, did not predict the observed intensities and dependence on τ.

The principal values of hf and nqi coupling parameters obtained from our computer simulations for substrate-derived nitrogen and the two nitrogens from TTQ, are listed in Table 1. Figure 6 shows the simulated frequency domain ESEEM spectra (dashed lines) calculated using the experimental conditions and τ values of 219 (Figure 6a), 365 (Figure 6b), and 450 ns (Figure 6c). The experimental ESEEM spectra are included in the figure (solid lines) for comparison. The simulations account well for the frequencies, relative amplitudes and line widths of the major ESEEM features. The trends in amplitude changes that occur with tau are also in agreement with experiment. The chief shortcomings of our modeling are in accounting for the details of the double quantum features. Independent information on the symmetries of the hyperfine tensors as determined from two-dimensional ESEEM measurements (HYSCORE)[31] would be beneficial here, but progress on such measurements has been impeded by the long T_{1e} of the MADH semiquinone (>1 s).

Close examination of the data shown in Figures 4 and 5 fails to reveal contributions from substrate-derived ^{15}N. To support this observation, simulations were done using the ^{14}N-coupling parameters given in Table 1 for the TTQ nitrogens along with ^{15}N hyperfine couplings obtained by scaling the corresponding

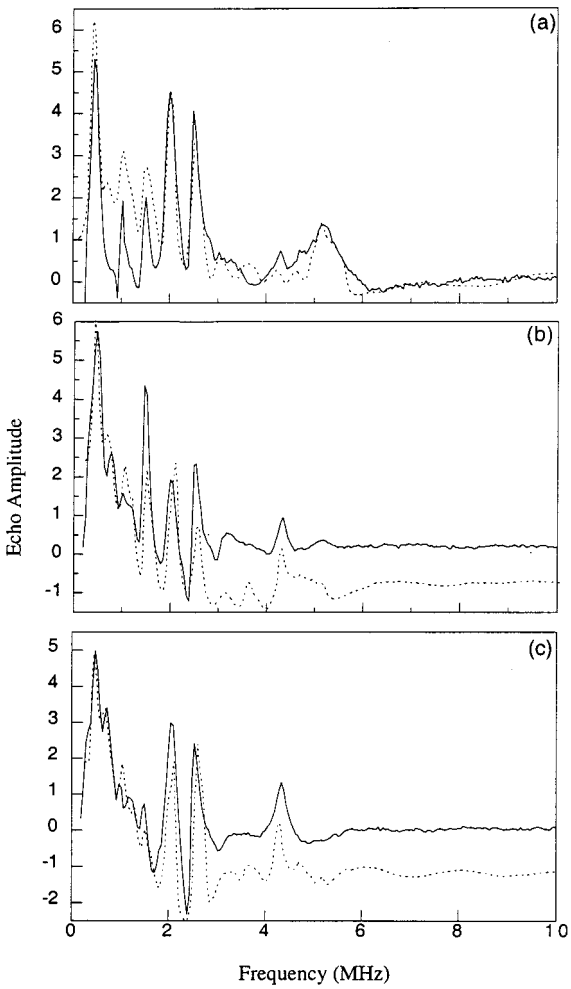

Figure 6. Cosine Fourier transformations of numerical simulations of three-pulse ESEEM data of $CH_3{}^{14}NH_2$-generated semiquinone in MADH (a) τ, 219 ns; (b) τ, 365 ns; (c) τ, 450 ns. The simulations (dashed lines) were performed using three coupled ^{14}N nuclei, N(1), N(2) and substrate-derived N, whose hf and nqi coupling parameters are listed in Table 1. Other simulation parameters: g_n, 0.4035; magnetic field strength, 315.5 mT. An isotropic electronic *g*-factor was assumed. The corresponding ESEEM data from Figures 4 and 5 are included for comparison (solid lines).

values measured for ^{14}N-substrate coupling. The results predicted that no distinct ^{15}N peaks would be resolved for ESEEM collected using the conditions of Figures 4 and 5. Simulations of 2-pulse data also showed that these measurements would not reveal ^{15}N contributions in the presence of deep modulation from the TTQ nitrogens.

Figure 7 shows a comparison of echo amplitude modulations for the time domain data collected at $\tau = 219$ ns for the ^{14}N-semiquinone (solid line), with that obtained from our simulation (dashed line). The simulation was multiplied by a decay function, $e^{-t/\tau}$, where τ was 4.5 μs. The depths of modulations in the time domain data and simulation agree well and show that the semiquinone is nearly pure N-form.

Our computer simulations made use of the spherical model approximation[32] to the product rule for assembling the ESEEM spectra of multiple, magnetically coupled nuclei. This approximation can be safely made for cases where there are at least four or more coupled nuclei. The consequences of this approximation were tested for dithionite-reduced MADH. For

(29) Cosgrove, S. A.; Singel, D. J. *J. Phys. Chem.* **1990**, *94*, 8393−8396.

(30) Dikanov, S. A.; Shubin, A. A.; Parmon, V. N. *J. Magn. Reson.* **1981**, *42*, 474−487.

(31) Dikanov, S. A.; Bowman, M. K. *J. Magn. Reson., A* **1995**, *116*, 125−128.

(32) Kevan, L.; Bowman, M. K.; Narayana, P. A.; Boeckman, R. K.; Yudanov, V. F.; Tsvetkov, Y. D. *J. Chem. Phys.* **1975**, *63*, 409−416.

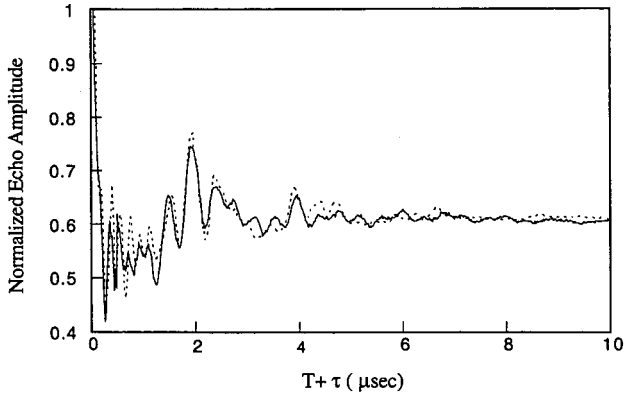

Figure 7. A comparison of the normalized three pulse electron spin−echo envelope modulation amplitudes for ^{14}N-methylamine poised MADH semiquinone measured experimentally (solid line) at $\tau = 219$ ns with that predicted by spectral simulation (dashed line) for the same tau value.

Table 2

	unpaired spin densities		
semiquinone	substrate	N(1)−TTQ	N(2)−TTQ
N-form	0.007	0.004	0.011
O-form	- - -	0.006	0.006

this case, only two nitrogens contribute to the data, and they do so in a nearly equivalent fashion.[19] To perform this task we modified our simulation software to simultaneously consider two $I = 1$ nuclei whose magnetic axes were related by a simple Euler angle rotation. If one considers the principal axes of both the hyperfine tensors to be at an angle of 45° with respect to one another, the ESEEM calculated with the precise formulation of the product rule yields results that are nearly identical with those obtained using the spherical model approximations. In the worst case, when both hyperfine principal axes are collinear or perpendicular, the errors made by using the spherical model approximation are modest. Because the X-ray crystal structure of MADH shows the planes of the indole and indole−quinone rings of oxidized TTQ to be at an angle of 38° with respect to each other, use of the spherical model approximation is justified for our work.

The above ^{14}N-ESEEM analysis has provided two types of Hamiltonian parameters that report on the electronic structure of the TTQ-semiquinone. The hyperfine coupling parameters can be directly related to the structure of the highest occupied molecular orbital (HOMO) of the semiquinone in that the dipolar portion of the tensors are a measure of the unpaired electron density localized in the p^{π}-orbital of each coupled nitrogen. A rough estimate of this pi-orbital unpaired spin density is obtained by dividing the A_{dip} values in Table 1 by the corresponding value measured for atomic nitrogen, 47.8 MHz. Table 2 summarizes the unpaired π-electron spin densities located on the three nitrogens coupled to N-form semiquinone and compares them to the values determined previously for the O-form radical.[19] All of the calculated p^{π} values are small, showing that our ^{14}N-ESEEM experiments are detecting only a small portion of the TTQ$^{\bullet}$ HOMO and that the HOMO is delocalized over the framework of the cofactor. However, these numbers do reveal some of the details of electronic structure changes triggered by substrate binding. For O-form semiquinone, the unpaired p^{π} spin densities on N(1) and N(2) nuclei of the cofactor are equal, consistent with a more uniform distribution. N-form semiquinone is characterized by an unpaired electron density on N(2) that is almost three times larger than that found for N(1). The presence of substrate-derived amine has altered the HOMO, increasing the contribution of N(2) to the MO while reducing that of N(1).

The alterations of the HOMO for the TTQ semiquinone caused by the presence of substrate-derived amine are interesting in the light of the different electron-transfer rates to amicyanin measured for N- versus O-form quinol and semiquinone intermediates of MADH.[33] Electron transfer from the N-semiquinone is slower than from the O-semiquinone. Conversely, electron transfer from the *N*-quinol, which yields the *N*-semiquinone as a product, is faster than from the O-quinol. The differences in the electron-transfer rates from the *N*- and O-semiquinone forms appear to be due to differences in their redox potentials.[33] The basis for differences in the reaction rates of the N- and O-form quinols, which yield the corresponding semiquinone forms as products, is more difficult to interpret because the reaction of the N-quinol is gated by the deprotonation of the substrate-derived amino group on TTQ[34] (discussed later). In addition to redox potential, two other parameters which determine electron-transfer rates are the electronic coupling (H_{AB}) and the reorganizational energy (λ).[35] H_{AB} is related to the distance that the electron must travel. An important result from this study is that the unpaired electron spin density in the TTQ semiquinone is delocalized over the framework of TTQ. This suggests that the starting point for the electron-transfer reaction may be any point on the cofactor, including the edge of the Trp108 indole ring, which is closest to amicyanin. The asymmetry of the spin density raises an interesting question of whether the observed differences in the HOMO for different TTQ forms would contribute to differences in H_{AB} for electron-transfer reactions from different redox forms. Another interesting question is to what extent does the electronic structure of the TTQ semiquinone, relative to that of the oxidized and reduced forms, contribute to the λ associated with electron-transfer reactions that involve the semiquinone TTQ as a reactant or product. The electron transfer reactions of MADH exhibit relatively large values of λ (>2 eV).[33] These new data will form the basis for future studies to elucidate any correlation between electron-transfer properties and the electronic properties of this and other organic redox cofactors.

The other group of ^{14}N-Hamiltonian parameters derived from this work are nuclear quadrupole interaction (nqi) parameters, e^2qQ and η. Although the ^{14}N nucleus has a small quadrupole moment, this interaction can often be substantial because of the large electric field gradient created by the atom's 2p electrons.[36] For the tricoordinate, planar geometries that describe the bonding of the ^{14}N nuclei of the TTQ semiquinone, the principal axis of the electric field gradient is directed along the $2p^{\pi}$ orbital of the atom, perpendicular to the three sp^2 hybrid orbitals that characterize the σ bonding. Using this simple Townes−Dailey description of the interactions, the value of e^2qQ, the quadrupole coupling constant, can be related to the electron occupancy of the nitrogen $2p^{\pi}$ orbital.[37] If this orbital houses 2 electrons, the e^2qQ value is >4 MHz. The e^2qQ value for the indole nitrogen of tryptophan powder is 3.0 MHz, which corresponds to a $2p^{\pi}$ orbital occupancy of about 1.75.[38] The e^2qQ values measured for the TTQ nitrogens of the O-form semiquinone are 3.0 (N(1))

(33) Bishop, G. R.; Davidson, V. L. *Biochemistry* **1998**, *37*, 11026−11032.
(34) Bishop, G. R.; Davidson, V. L. *Biochemistry* **1997**, *36*, 13586−13592.
(35) Marcus, R. A.; Sutin, N. *Biochim. Biophys. Acta* **1985**, *811*, 265−322.
(36) Lucken, E. A. C. *Nuclear Quadrupole Coupling Constants*; Academic Press: London, 1969.
(37) Townes, C. H.; Dailey, B. P. *J. Chem. Phys.* **1949**, *17*, 782−796.

and 3.2 (N(2)), indicating that the occupancy of the p^{π} orbital on these heteroatoms is not greatly affected by the protein environment or the difference between the electronic structure of the cofactor and the amino acid model compounds.

The other nqi parameter, η, is termed the asymmetry parameter and is used to describe the degree of rhombicity in the electric field gradient. η ranges from 0, for an axial interaction, to 1 for the completely rhombic case.[36] For tryptophan powders, the indole nitrogen is found to have $\eta = 0.18$ indicative of an axial tensor and a measure of the "equivalence" of the C−N and N−H bonds. For the O-form semiquinone, Warncke et al. found that η for N(1) was 0.2, identical to that of the tryptophan model, while the N(2) asymmetry was 0.6, indicating an asymmetry likely caused by hydrogen-bonding to the peptide. The X-ray crystal structure of oxidized MADH shows nearly equivalent hydrogen bonding interactions for both the indole and the indole−quinone nitrogens.[5] The results of Warncke et al. on O-form semiquinone show that only one of these interactions is important for reduced cofactor.[19]

The differences observed in ^{14}N hyperfine couplings between O- and N-form semiquinones are mirrored by changes in e^2qQ. For the N(1) nitrogen of N-form TTQ$^{\bullet}$, both e^2qQ and η were determined to be 3.0 and 0.3, respectively, and were found to remain close to the indole model compound values. The e^2qQ values for the N(2) nitrogen dropped from 3.2 MHz for the O-form to 2.1 MHz for the substrate-reduced enzyme. Using the analysis results of Edmonds and Speight, this decrease in e^2qQ can be interpreted as a decrease in the N(2) $2p^{\pi}$ orbital population from ~1.75 to about 1.63. This decrease is supportive of our ESEEM simulation results for N(2) that attribute the lack of a "double quantum" peak to an increase in hyperfine anisotropy or $2p^{\pi}$ unpaired electron spin density. The asymmetry parameter for N(2) was found to be nearly 0.7, essentially unchanged from the value determined for the O-form.

The ESEEM spectra of the N-form semiquinone also yielded a well-resolved set of resonances due to substrate derived nitrogen. The measured isotropic coupling constant is 2.4 MHz, in good agreement with value estimated from samples prepared by comproportionation and studied previously by ESEEM.[13] This value compares well to those measured for the TTQ nitrogens, 2.7 (N(1)) and 1.9 (N(2)), and definitely shows that the substrate-derived nitrogen is covalently bound to the TTQ semiquinone. The low value of e^2qQ, 1.7 MHz, and the deviation of the asymmetry parameter from that expected for an axial interaction ($\eta = 0.5$) are commensurate with the incorporation of the substrate nitrogen into the π-system of the TTQ semiquinone and our previous proposal that the nitrogen is an imine-like species.[10,34] The low value of e^2qQ dictates that all of the substrate-derived nitrogen's electrons are involved in bonding interactions and agrees well with the e^2qQ value determined for the substrate-derived nitrogen of the topa-semiquinone cofactor of copper amine oxidases.[39,40] For these systems a combination of ^{14}N- and ^{2}H-ESEEM and ^{1}H-ENDOR spectroscopies were used to show that the nitrogen derived from amine substrate was bound to the topa-quinone cofactor as an imine-like species with one strongly- and one weakly coupled exchangeable proton accounting for the bonding about the heteroatom.[40]

For MADH, an imine-like semiquinone species with one strongly- and one weakly coupled exchangeable proton is very consistent with the chemical reaction mechanism that we have proposed for the deprotonation reaction that gates the electron transfer from the N-quinol MADH to amicyanin.[34] It was proposed that rate-limiting deprotonation of the substrate-derived amino group on reduced TTQ was required to activate the system for rapid electron transfer. This deprotonation of TTQ-bound $-NH_2$ requires a monovalent cation at the active site to stabilize the transient $-NH^-$ intermediate from which electron transfer occurs to yield the $=N-H$ imino-semiquinone product. Thus, in the semiquinone state the active site residue which removed the proton from $-NH_2$ will still be in close proximity to the $=N-H$ of the semiquinone and in a position to provide this same proton for hydrogen bonding to the imino−semiquinone nitrogen. This would yield one strongly (covalent), and one weakly (H-bonded) coupled exchangeable proton.

Conclusions

The ESEEM experiments and analyses presented in this paper show that the semiquinone species obtained by light-induced oxidation of substrate-reduced MADH contains a covalently bound nitrogen atom that is derived from substrate methylamine. The nuclear quadrupole coupling constant, e^2qQ, measured for this substrate-derived nitrogen is consistent with that determined for the topa-semiquinone species of amine oxidases[39] and is very distinct from the value measured for methylamine by NQR spectroscopy.[36] It is likely that this substrate-derived nitrogen exists as imine nitrogen in the TTQ semiquinone, with the lone pair of electrons that reside in the remaining sp^2 hybridized orbital involved in the formation of a strong hydrogen bond with an available proton-donor. Furthermore, the match between the depths, or intensities, of the ESEEM predicted by our simulations and the experimental data provides strong evidence that the intermediate species prepared, using the light-induced oxidation procedure developed by Zhu and Davidson,[21] is pure N-form semiquinone. It is important to note that these results were obtained using stoichiometric amounts of substrate reacted with enzyme rather than the 10^4-10^6 molar excesses that are typical in cation binding studies.[14−16]

The broadening of the cw-EPR line shape found for substrate-reduced semiquinone when compared to that of dithionite-reduced enzyme reflects changes in the electronic structure of TTQ$^{\bullet}$ that are a consequence of the substitution of substrate nitrogen for the C6 oxygen atom. The hyperfine couplings measured in this work for the three nitrogen atoms of the semiquinone provide details of how the highest occupied molecular orbital of this chemical intermediate are affected by substrate addition. Further characterization of this species by proton ENDOR spectroscopy will provide a detailed picture of the HOMO and key information for understanding how the electronic structure of the TTQ semiquinone in MADH effects the rates and mechanisms of electron transfer from different redox forms of MADH to amicyanin.

Acknowledgment. This work was supported by funds from National Institutes of Health, Grants GM-54065 (JLM) and GM-41574 (VLD).

JA9934246

(38) Edmonds, D. T.; Speight, P. A. *J. Magn. Reson.* **1972**, *6*, 265−273.

(39) McCracken, J.; Peisach, J.; Cote, C. E.; McGuirl, M. A.; Dooley, D. M. *J. Am. Chem. Soc.* **1992**, *114*, 3715−3720.

(40) Warncke, K.; McCracken, J.; Babcock, G. T.; McGuirl, M. A.; Dooley, D. M. *J. Am. Chem. Soc.* **1994**, *116*, 4028−4037.